Synthesis, Spectra, and Electron-Transfer Reaction of Aspartic Acid-Functionalized Water-Soluble Perylene Bisimide in Aqueous Solution

Lina Zhong, Feifei Xing,* Wei Shi, Liuming Yan, Liqing Xie, and Shourong Zhu*

Department of Chemistry, College of Science, Shanghai University, Shanghai 200444, China

Ⓢ *Supporting Information*

ABSTRACT: An aspartic acid-functionalized water-soluble perylene bisimide, N,N'-di(2-succinic acid)-perylene-3,4,9,10-tetracarboxylic bisimide (PASP) was synthesized and characterized. It has absorbance maximum A^{0-0} and A^{0-1} at 527 and 498 nm ($\varepsilon \approx 1.7 \times 10^4$ L cm^{-1} mol^{-1}) respectively in pH 7.20 HEPES buffer. Two quasi-reversible redox processes with $E_{1/2}$ at -0.17 and -0.71 V (vs Ag/AgCl) respectively in pH 7−12.5 aqueous solutions. PASP can react with Na$_2$S in pure aqueous solution to form monoanion radical and dianion species consecutively. PASP$^{-\bullet}$ has EPR signal with $g = 1.998$ in aqueous solution, whereas PASP^{2-} is EPR silent. The monoanion radical formation is a first-order reaction with $k = 8.9 \times 10^{-2}$ s^{-1}. Dianion species formation is a zero-order reaction and the rate constant is 4.3×10^{-8} mol L^{-1} s^{-1}. The presence of H$_2$O$_2$ greatly increases the radical formation rate constant. PASP as a two-electron transfer reagent is expected to be used in the water photolysis.

**KEYWORDS:** *perylene bisimide, electron transfer, anion radical*
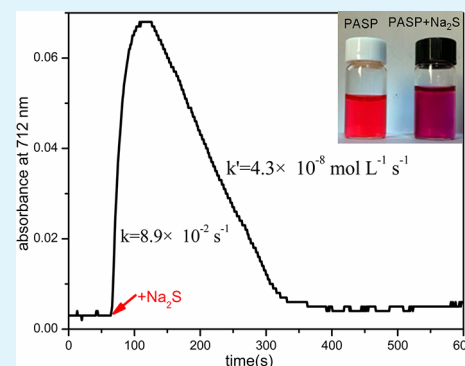
INTRODUCTION

Because of unique light-harvesting[1] and redox properties[2] as well as high chemical persistency, thermal durability, and photostability,[3] perylene dyes have been regarded as potential candidates for numerous applications.[4−13] Perylene dyes continue to emerge as archetypal components in a variety of photo functional materials. Among the derivatives of perylene dyes, the perylene bisimide (PDI) dyes seem to be ideal for light-based applications because of their excellent photophysical properties.[14−24] Perylene bisimides are one of the hot topics in current chemical research. This type of PDI dyes have strong absorption with high molar absorption coefficients ($\varepsilon = 58\,000$ M^{-1} cm^{-1}) at 490 nm in CHCl$_3$, a long fluorescence lifetime, near-unity fluorescence quantum yields.[3] PDIs present a chemical versatility to introduce new substituents from imide groups and the bay region (positions 1, 6, 7, and 12) to overcome their inherent low solubility[25] and adjust spectral and electrochemical properties.[3,26] Of the commonly used substituents, amino acids, such as alanine,[27] serine,[28] aspartic acid,[29−33] histidine,[34] and lysine,[35] were one kind of the convenient choices to increase water solubility of PDIs. Besides spectrum, the other most important properties are related to the facile reduction of PDI derivatives, giving relatively stable radical anion species. The electron acceptor character is a common property of aromatic diimides[36] and arises from the strong electron-withdrawing power of the imides groups. PDIs can be easily reduced in two steps, generating monoanion radical, followed by doubly reduced to dianion.[37] In the literature, electrochemical or photochemical reduction was employed to study the properties of PDIs in organic solvents, such as ethanol,[37] CH$_2$Cl$_2$-TEA,[36] DMF,[38] etc. Marcon etc have

studied the electron-transfer reaction between PDIs and sodium dithionite (Na$_2$S$_2$O$_4$) in water, ethanol, and ethanol/water solvent that the formation of monoanion radical and dianion were observed in these solutions.[37,39,40] Hydrazine was also used in PDIs reduction.[38] However, there is much less information available on the reduction of PDI, especially in pure aqueous solutions.

Reductant Na$_2$S is less active than Na$_2$S$_2$O$_4$. There are no precedence of the interaction between PDIs and Na$_2$S. Herein, we report the synthesis of water-soluble perylene bisimide PASP (Scheme 1) and its electron-transfer reaction with Na$_2$S.

Scheme 1. Structure of N,N'-Di(2-succinic acid)-perylene-3,4,9,10-tetracarboxylic Bisimide (PASP)
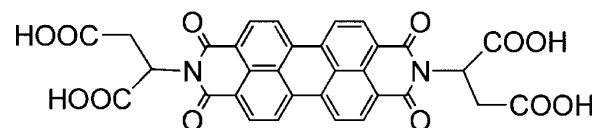
EXPERIMENTAL SECTION

Materials. 3,4,9,10-Perylenetetracarboxylic dianhydride was purchased from Shanghai TCI (shanghai, china). Aspartic acid (ASP), imidazole and all other inorganic reagents are A.R grade from Sinopharm Chemical Reagent Co, Ltd. Shanghai. 4-(2-Hydroxyethyl)-1-piperazineethanesulfonic acid (HEPES) was supplied by Aladdin Co,

Ltd. (Shanghai, China). All chemical regents were used as obtained without further purification. Solutions were prepared with sub-boiled water distilled in all-quartz apparatus.

Characterization. ^{1}H NMR spectrum was measured on Bruker AV 500 MHz spectrometer. Infrared spectrum was recorded on a Nicolet A370 FTIR spectrometer using KBr pellets in 4000−400 cm^{-1} region. The elemental analyses (C, H and N) were obtained on a Vario EL III analyzer. UV−vis absorption spectra were performed with a Puxi TU-1900 spectrometer with a 1.0 cm quartz cell equipped with a temperature-controlled water bath (25 °C). Electron paramagnetic resonance (EPR) spectra were recorded by a JES-FA 200 spectrometer, fitted with the DICE ENDOR accessory, EN801 resonator, and an ENI A-500 rf power amplifier. Cyclic voltammograms (CV) were carried out on CHI660A instrument. Glassy carbon working electrode, a platinum wire counter electrode, and a reference electrode Ag/AgCl were employed.

Molecular-Orbital Calculation Method. The density functional theory (TDDFT) calculations were used to investigate the absorbance characteristics of PASP at B3LYP/6-31G (D) level of theory with the PCM model applied as implemented in the GAUSSIAN 03 program.[41] Both the neutral PASP and the reduced PASP anion were optimized, and were verified to be local minimum by frequency calculations (without imaginary frequencies). And the absorbance characteristics were calculated using the time-dependent density functional (TDDFT) theory at the same level of theory.[42]

Synthesis of *N,N′*-Di(2-succinic acid)-perylene-3,4,9,10-tetracarboxylic Bisimide (PASP). PASP was prepared in a similar way to literature method.[8] 3,4,9,10-perylenetetracarboxylic acid bisanhydride (392.8 mg, 1.0 mmol), aspartic acid (273.4 mg, 2.05 mmol), and 4.000 g of imidazole were added into a flask and heated to 160 °C for 8 h with stirring under N$_2$ atmosphere. The reaction mixture was allowed to cool to room temperature, and then 100.0 mL hot water was poured into the reaction flask. Insoluble impurities were filtered and discarded. To the aqueous solution was added 250.0 mL 2.0 M HCl, then the precipitate was centrifuged and washed twice with water and ethanol, respectively. The solid was dried under vacuum at 80 °C to give the crude product. The crude product was further purified by dissolving in 50.0 mL DMF then add 2.0 M HCl to adjust pH ∼1; dissolving in 50.0 mL KOH solution (4.5 mmol, 252.5 mg) and then precipitated by dropwise adding of 0.12 M HCl to pH ∼1. Precipitation was washed twice with ethanol and then dried under vacuum at 80 °C to give the product of PASP·5H$_2$O (451.9 mg, 63.42%). FTIR (KBr) ν/cm^{-1}: 3455, 2941, 1755, 1656, 1642, 1592, 1575, 1508, 1435, 1401, 1365, 1347, 1302, 1255, 1178, 1132, 1026, 994, 960, 864, 810, 748, 643, 545, 510, 470, and 435 cm^{-1} (see Figure S1 in the Supporting Information). [1]H (500 MHz, d$_6$-DMSO,) δ: 12.85 (s, 2H), 7.91 (t, 4H), 7.75 (d, 4H), 5.99 (m, 2H), 3.38 (m, 2H), 2.90 (m, 2H) (see Figure S2 in the Supporting Information). UV−vis (H$_2$O): λ_{max} (ε) = 527 (1.7×10^4) and 498 nm (1.7×10^4 M^{-1} cm^{-1}). Anal. Calcd for C$_{32}$H$_{18}$O$_{12}$N$_2$·5H$_2$O: C, 53.80; H, 3.539; N, 3.924. Found: C, 53.9376; H, 3.9606; N, 3.9313. Details and information related to further purification were given in the Supporting Information.

■ RESULTS AND DISCUSSION

Absorption Spectra of PASP. PASP exhibits good solubility in alkali aqueous due to the electrostatic repulsion between its multiple negative charges. Since PDIs have strong aggregation tendency which will change their absorption spectra. The absorption spectra of PASP in HEPES buffer (50 mM, pH 7.20) over a wide concentration range of 0.1 to 80 μM were recorded as shown in Figure 1. The spectrum shows two absorption bands (527 nm, 498 nm) and two broad shoulder peak around 469 and 436 nm, which corresponding to the characteristic of the 0−0, 0−1, 0−2, and 0−3 transition energy, respectively (0−0 means the transition from grand state to zero energy level of excited state, 0−1, 0−2, 0−3 means the
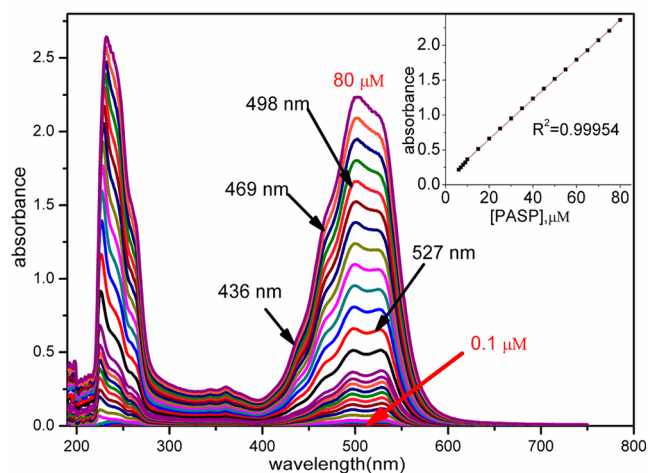

Figure 1. Absorption spectra of 0.1−80 μM PASP in HEPES buffer (50 mM, pH 7.20). Inset: Plots of absorption versus concentration of PASP at 498 nm.

transition from grand state to the first, second, and third excited state, respectively).[43]

The large conjugate aromatic ring has strong tendency of aggregation via $\pi-\pi$ and/or hydrophobic interaction in aqueous solution. According to the literature,[44] monomer PDIs exhibit normal Franck−Condon progression with the ratio of 527 and 498 nm UV-vis absorption $A^{0-0}/A^{0-1} \approx 1.6$ (A^{0-0} means the absorbance of transition from grand state to zero energy level of excited state, A^{0-1} means the absorbance of transition from grand state to the first excited state), whereas aggregated molecules have inversed intensity distribution with $A^{0-0}/A^{0-1} \leq 0.7$. The A^{0-0}/A^{0-1} of PASP in aqueous solution varies from 1.1 at 0.1 μM to 0.9 at 80 μM. (Figure S3, see the Supporting Information). From these data, it can conclude that increase PASP concentration will decrease the ratio of A^{0-0}/A^{0-1}. The good linear relationship between absorption intensity (both 527 and 498 nm) and the concentration of PASP ($R^2 = 0.99954$ from 0.1 to 80 μM) indicated that either the monomer and aggregation were insignificant, or the absorption coefficients of PASP in monomer or aggregates were similar in HEPES. The lowest detectable concentration of PASP speculated from Figure 1 was 0.1 μM.

As we all know that the form, and thereof the spectra of a weak acid depends on pH.[45] Figure 2 is the absorption spectra of 10 μM PASP from pH 6.92 to 12.54. PASP is essentially insoluble in pH <6.2. The absorbance at 527 nm increases according to the increase of pH from 8.52 to 11.92 region ($R^2 = 0.99467$) (Figure 2, inset). Below pH 7.20, the absorbance at 527 nm decreases sharply. It was reported that succinic acid has pK_{a1} and pK_{a2} of 4.21 and 5.64, respectively.[46] Minimum pH to remove both protons from succinic acid is ∼pH 7.64, which agrees well with the high absorbance in pH range of 7.5−12 in aqueous solution. PASP contain two succinic acid substitutes, fully deprotonate PASP needs higher pH (>7.64). There is still some aggregations in pH 7.20−8.52. Aggregation reaction (from monomer) is quite slow compared with deprotonation reaction, this may explain why 527 nm absorbance do not increase with the increases of pH in 7.20−8.52. The absorbance of PASP at 527 nm slightly increases with the increase of pH in pH > 8.5, which indicates the negative charges in the aspartic moiety disfavor aggregation form of PASP. However, the $A^{0-0}/$
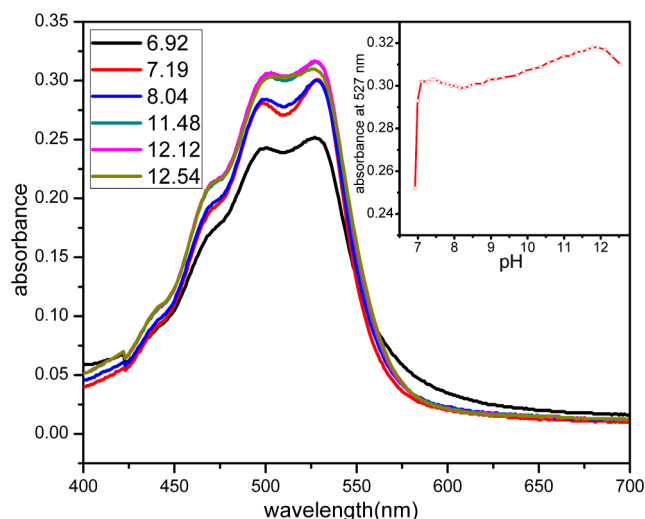
Figure 2. Absorption changes of PASP (10 μM) at different pH in HEPES buffer (50 mM). Inset: Dependence of the absorption of PASP at 527 nm at different pH in HEPES buffer (50 mM).

A^{0-1} is 1.03 to 1.05 in pH 8.5−12.5, which indicates no observable aggregation changes in basic aqueous solution.

Electrochemistry Properties of PASP. The redox behavior of PASP was analyzed by cyclic voltammetry (CV). Figure 3 showed the cyclic voltammetry of PASP (1.0 mM) in
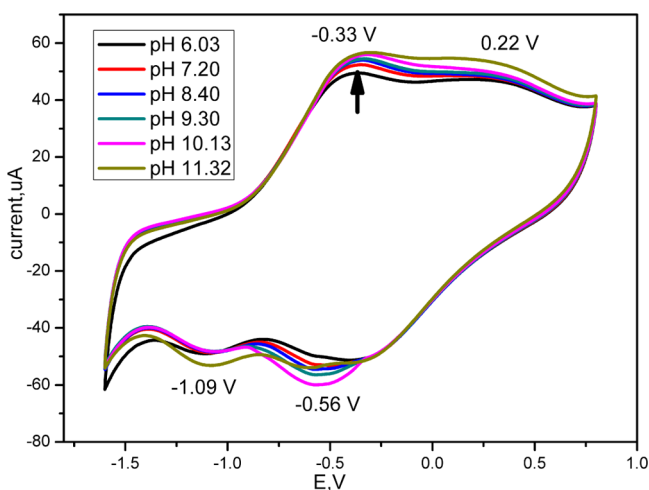

Figure 3. Cyclic voltammograms of 1.0 mM PASP in 0.1 M Na_2SO_4 aqueous solution at different pH (V, vs Ag/AgCl). The scan rate was 200 mV/s.

0.1 M Na_2SO_4 aqueous solution in pH 6.03−11.32. Two oxidation peaks at $E_{p,a}$= −0.33 and 0.22 V (vs Ag/AgCl), and two reduction peaks $E_{p,c}$= −1.09 V and −0.56 V (vs Ag/AgCl) were observed. The quasi-reversible reduction and oxidation peaks at the negative potentials, which indicated PASP was a good n-type materials.[47] The half-potentials of −0.17 V and -0.71 V (vs Ag/AgCl) were calculated from Figure 3 corresponding to the formation of monoanion radical PASP$^{-•}$ and dianion PASP^{2-}. No discernible CV graphs change observed between pH 6−11.3. From the relationship between scan rate and peak current, the reduction process is quasi-reversible (see Figure S4 in the Supporting Information). The half-wave potentials ($E_{1/2}$) of PDI derives in different solvents were summarized in Table 1. The $E_{1/2}$ value of PASP was −0.13

Table 1. Half-Wave Potentials of PDIs (V vs SCE)

compd	solvent	$E_{1/2}^{0/-}$	$E_{1/2}^{-/2-}$	ref
1[a]	CH_2Cl_2	−0.46	−0.68	48
2[b]	CH_2Cl_2	−0.41	−0.66	48
3[c]	toluene/CH_3CN(4:1)	−0.76	−0.77	49
4[d]	CH_2Cl_2	−0.50	−0.73	50
5[e]	CH_2Cl_2	−0.63		50
6[f]	CH_2Cl_2	−0.55		47
7[f]	CH_2Cl_2	−0.75		47
8[f]	CH_2Cl_2	0.77		47
PASP	water	−0.13[g]	−0.67[g]	this paper

[a]1 is 1,6-difluoride substituted PBI-F$_2$.[48] [b]2 is 1,6,7,10-tetrafluoride substituted PBI-F$_4$.[48] [c]3 is N,N′-di(10-nonadecyl)perylene-3,4,9,10-tetracarboxylic diimide.[49] [d]4 is N,N′-di(C$_8$H$_{17}$)$_2$-perylene-3,4,9,10-tetracarboxylic diimide.[50] [e]5 is N,N′-di (2-ethylhexyl)$_2$-perylene-3,4,9,10-tetracarboxylic diimide.[50] [f]Compounds 6, 7, and 8 are P(BDT-PDI), P(BDT-NDI) and P(BDT-PhI).[47] [g]$E_{1/2}$ (vs SCE) = $E_{1/2}$ (vs Ag/AgCl) + 0.0443.

V (vs SCE) in aqueous solution that was larger than most other PDIs in organic solvents, indicating PASP can be relatively easily reduced to monoanion radical and dianion. The PASP radicals should be more stable than most other PDI radicals.

Electron-Transfer between PASP and Na$_2$S in Aqueous Solution. As PDIs are good n-type semiconductor materials, they can accept electrons to give anionic radical. Accordingly, the PDIs can be easily reduced in two steps, generating monoanion radical and dianion species consecutively.[51,52] The reductants used were hydrazine,[38] OH$^-$ in deaerated acetonitrile,[53] sodium dithionite ($E^θ$ = −1.12), etc., in the literature.[41,54,55] As discussed above, PASP has relatively larger $E_{1/2}$ compared to other PDIs listed in Table 1. Here we investigated the electron transfer between PASP and Na$_2$S ($E^θ$= −0.48 V). To the best of our knowledge, there is no precedence of reduction between Na$_2$S and PDIs.

As shown in Figure 4, the addition of 0.1 M Na$_2$S to 10 μM PASP aqueous solution leads to the formation of the corresponding monoanion radical PASP$^{-•}$, with absorptions maximum at 712 nm ($\varepsilon = 7.2 \times 10^3$ L cm^{-1} mol^{-1}) and 803 nm ($\varepsilon = 3.4 \times 10^3$ L cm^{-1} mol^{-1}), consistent with the values
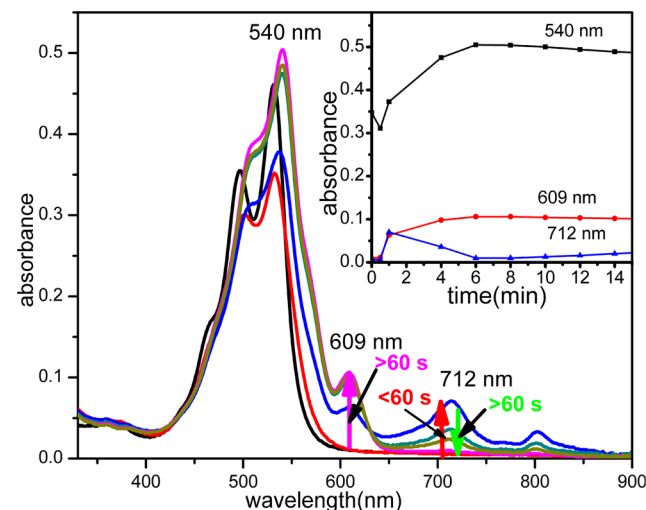
Figure 4. UV−vis absorption spectra changes and dynamic curve at absorption 540, 609, and 712 nm of 10 μM PASP with 0.1 M Na$_2$S in pH ∼12 aqueous solution at different times before shaking.

3403

dx.doi.org/10.1021/am4004446 | ACS Appl. Mater. Interfaces 2013, 5, 3401−3407

Table 2. Absorption Maxima (nm(ε)) for Some PDIs in the Ground State and Reduced Forms in Different Solutions

Compound	Solvent	Reductant	Non-radical	Radical anion	Dianion	Ref
	water/ethanol 1:1(v/v)	$Na_2S_2O_4$	527 (50000) 473 (40000)	960 800 (20000) 713 (40000)	650 (15000)	39
Zirconium phosphonate films	ethanol	$Na_2S_2O_4$	527 (50000) 473 (40000)	987 (3000) 818 (3000) 728 (4000)	650 (shoulder)	39
	water	$Na_2S_2O_4$	540 (18500) 500 (36200)	987 (18200) 817 (15400) 730 (24800)	600 (18300) 536 (74500) 506 (47000)	14
	water/ethanol 1:1(v/v)	$Na_2S_2O_4$	528 (59600) 492 (46700)	960 (26500) 800 (39500) 713 (84000)	601 (20100) 537 (76500) 503 (46400)	14
	ethanol	OH^-	530 ($\sim10^5$)	713 ($\sim10^5$)	600 ($\sim10^5$) 546 ($\sim10^5$)	53
	water	Na_2S	527 (17000) 498 (17000)	803 (3400) 712 (7200)	609(10000)	this paper

($Na_2S_2O_4$ as reductant) reported by Marcon etc (summarized in Table 2).[37,39,40] The absorptions at 712 and 803 nm increase in the first 60 s, which represents the generation of monoanion radical PASP$^{-\bullet}$. In the first 60 s, the 540 nm absorbance decreased 17%. The reduction of PASP to PASP$^{-\bullet}$ in water proceeded only until ca. 17% of PASP had been reduced (Figure 4, inset). After 60 s, absorption at 712 and 803 nm decreases with new peak at 609 nm (dianion PASP$^-$, $\varepsilon = 1.0 \times 10^4$ L cm^{-1} mol^{-1}) increases. The spectra of PASP^{2-} are also in agreement with the reported spectra (Table 2).[37,39] When time was longer enough, all the absorbance at wavelengths longer than 650 nm vanished and the absorbance at 609 nm increases to the maximum, indicating that PASP$^{-\bullet}$ was quantitatively reduced to PASP^{2-}. Aggregation will prevent the reduction from radical anion to dianion because of spin pairing.[56,57] The color of PASP solution changed from pink to red monoanion radical after adding Na_2S aqueous solution (Figure 5, inset). Purple dianion formed 60 s later, which were highly stabilized in aqueous solution at room temperature in air in the presence of Na_2S (without vigorous shaking). However, the purple

dianion solution fades quickly to original pink after vigorous shaking the solution in air. The UV−vis spectra were identical to those before shaking (see Figure S5 in the Supporting Information). A reasonable explanation for this phenomenon is that the purple PASP^{2-} was oxidized to PASP by O_2 in the air.

Figure 5 shows the dynamic traced curve of PASP at 712 nm, which clearly represented the formation process of monoanion radical and dianion are a continuous reaction. According to the firs-order reaction, $kt = \ln[(A_\infty - A_0)/(A_\infty - A_t)]$, where k is the first-order rate constant, A_∞, A_t, and A_0 are the 712 nm absorbance at time ∞, t, and 0. Plots of $\ln[1/(A_\infty - A_t)]$ vs t give a straight line for the formation of monoanion radical at the first 30 s. The slope of the line is rate-constant k. The k for the radical anion formation is 8.9×10^{-2} s^{-1} ($R^2 = 0.99574$). The 712 nm absorbance decreases linearly during the time period of 40−300 s. This indicates the formation of dianion is a zero-order reaction. Zero-order reaction rate constant is 4.3×10^{-8} mol L^{-1} s^{-1} ($R^2 = 0.99786$). The $t_{1/2}$ of the monoanion radical formation is about 10 s, whereas $t_{1/2}$ of its consumption is about 100 s.

The monoanion radical was also measured by electron paramagnetic resonance (ESR) spectrometry as shown in Figure 6. Free PASP aqueous solution is EPR silent. In the presence of Na_2S, anion radical PASP$^{-\bullet}$ generated immediately. The symmetric spectra with g-tensor of 1.998 were observed for monoanion radical, which is similar to the literatures except for the EPR fine structure.[36,56,57] Subsequent reduction to generate PASP^{2-} will take place at longer reaction time, results in an EPR silent species. This indicates that the electrons in dianion PASP^{2-} paired in the PASP orbital results in the disappearance of EPR signal. It can be seen that the signals are weaker gradually, even to disappear when PASP$^{-\bullet}$ was completed reduced to PASP^{2-}. These results agree well with the literature.[58]

As mentioned above, the monoanion radical will disappear upon vigorous shaking in air atmosphere. We believe it is the air oxygen that oxidized monoanion radicals into nonradical molecules (see Figure S5 in the Supporting Information). Reaction with oxygen will generate H_2O_2, so we studied the reaction of PASP and Na_2S in the presence of H_2O_2. We expect that H_2O_2 may oxidize monoanion radicals and then regenerate free PASP molecules. Beyond our expectation, when H_2O_2
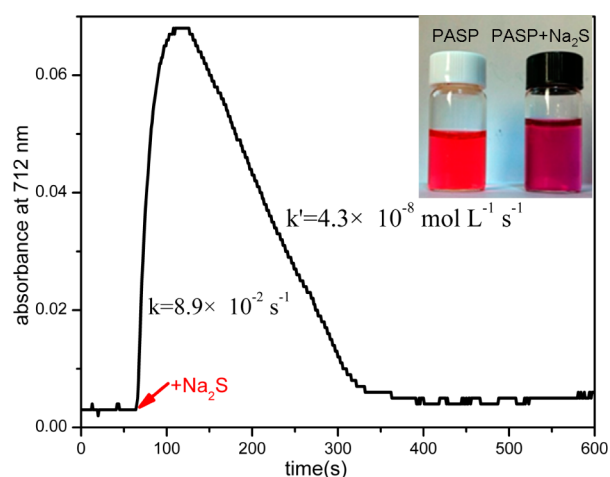

Figure 5. Dynamic curve of 712 nm absorption of PASP (10 μM, pH 7.2) in the presence of Na_2S (0.1 M, pH 12) aqueous solution at 25 °C. Inset: Photograph of PASP aqueous solution in the absence and presence of Na_2S.
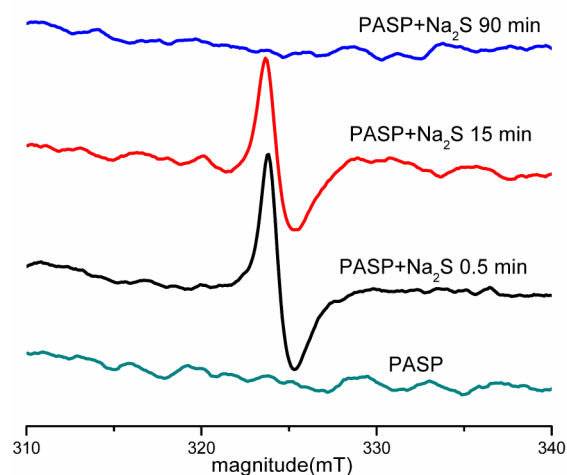
Figure 6. Comparison of X-band EPR spectra of PASP (10 μM) in the presence of Na$_2$S (0.27 M) aqueous solution at different time. The temperature was 213.5 K. The microwave power was 2 mW with the modulation amplitude of 1T at 100 kHz.

Figure 7. First three excitations of the neutral PASP with a PCM model applied.

(1.47 mM) was added to the solution of 10 μM PASP and 0.1 M Na$_2$S (pH∼12), the reaction of monoanion radical formation and dianion formation were prominently increased. H$_2$O$_2$ cannot oxidize PASP anion radical in pH 12 aqueous solutions. The reduction in the presence of H$_2$O$_2$ and Na$_2$S is so fast that the intermediate, monoanion radical, absorbance at 712 nm, could not be observed in the presence of 1.47 mM H$_2$O$_2$ (see Figure S6 in the Supporting Information). The 609 nm dianion formation was also much faster that the reaction completed within 1 min. The UV−vis changes were identical to that system without H$_2$O$_2$, except that it changed more rapidly from pink to purple almost in several seconds. Figure S7 (Supporting Information) showed the EPR spectrum of 10 μM PASP in the presence of in 0.27 M Na$_2$S and 1.47 mM H$_2$O$_2$ in aqueous solution (immediately). Then the EPR signal disappeared within a few minutes. This agrees with the phenomena that H$_2$O$_2$ could speed up the reduction of PASP. It worthy to mention that when 0.15 M H$_2$O$_2$ was introduced into 10 μM PASP aqueous solution at pH 9−12 (pH values were adjusted by using 0.1 and 5 M NaOH), the UV−vis spectra have no changes within a long time. This indicates that H$_2$O$_2$ itself cannot reduce PASP at all. A plausible explanation is that $E_B(O_2/H_2O_2)$ = −0.146 V, which is slightly lower than $E_{1/2}$ = −0.13 V, indicates that H$_2$O$_2$ may be a catalyst in PASP reduction. However, −0.146 V is not low enough to reduce PASP. In the absence or presence of H$_2$O$_2$, the dianion could exist stably. PASP as a two-electron transfer reagent is expected to be used in the water photolysis application and electron transfer aspects.

Molecular-Orbital Calculation. From the TDDFT calculation, the first excitation of PASP from HOMO to LUMO with a wavelength of 546.1 nm with oscillation strength of 0.94 calculated with a PCM model applied, which is also the essential light-absorbing excitation. This data agrees well with 527 nm absorption in aqueous solutions. The next two excitations are mixing states from HOMO−1 to LUMO and HOMO−2 to LUMO as shown in Figure 7, in good agreement with literature for the second excitation while disagreement for the third excitation.[32] These calculated excitation energies show good agreement with our experimental spectra of PASP in aqueous solution. Tables S1 and S2 in the Supporting
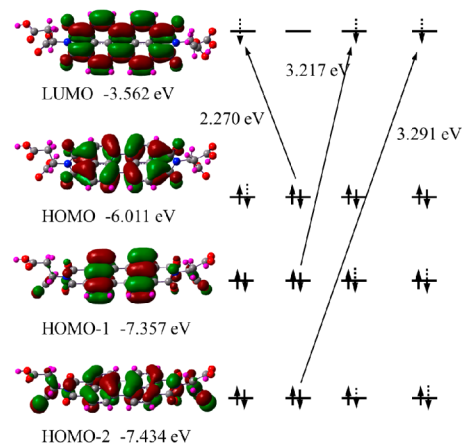
Information summarize the first eight excitations of the neutral PASP and the first three excitations of the reduced PASP anion calculated by TDDFT without and with the PCM model applied. From the PCM model, the wavelengths of the first three excitations of the PASP anion radicals are at 855.5, 678.3, and 628.4 nm, and the third excitation is the essential excitations with oscillation strength of 1.04. These data are somewhat different from solution absorbance at 803 and 712 nm, possibly due to the anion radical has much strong interaction with solvents than that of the neutral molecules. Table 3 summarized the absorbance energy and corresponding wavelengths calculated by TDDFT without and with PCM model applied and experimental data.

Table 3. Comparison of the Absorbance Data between Experimental and TDDFT Calculation

	TDDFT				experimental data	
	PCM		gaseous phase			
	eV	nm	eV	nm	eV	nm
neutral	2.27	546.1	2.39	518.8	2.35	527
	3.22	385.1	2.641	469.5	2.64	469
	3.29	376.9	2.801	441.4	2.84	436
anion radical	1.45	855.5	1.46	850.5		
	1.83	678.3	1.85	669.0	1.54	803
	1.97	628.4	2.09	594.0	1.74	712
dianion					2.04	609

The difference between the $E_{1/2}$ of ferrocenium-ferrocene and Ag/AgCl is 0.18 V. The HOMO (IP) and LUMO (EA) are: LUMO = −[($E_{1/2\ red1}$ vs Ag/AgCl) + 4.62] = −4.45 eV.[59] The HOMO values were estimated to be HOMO = LUMO − E_g = −6.80 eV, using the optical band gap calculated from the formula: E_g^{opt} = 1240/λ$_{max}$ = 2.35 eV (527 nm). The experimental $E_{1/2}$ from CV in aqueous solution agree well with PCM calculation (LUMO = −3.562 eV, HOMO = −6.011 eV). The LUMO energy levels of −4.45 eV and the two negative reduction potentials suggest that PASP was a typical n-type polymer that could be used as electron acceptors in all polymer solar cells.[47]

CONCLUSION

An aspartic-acid-functionalized water-soluble perylene bisimide PASP was synthesized and characterized. Aqueous solution absorption spectra were studied at different concentrations and pH values. PASP can react with Na_2S in aqueous solution to form monoanion radical and dianion. The monoanion radical has EPR signal, while the dianion was EPR silent. The formation of monoanion radical was a first-order reaction, whereas dianion formation was a zero-order reaction. The electron-transfer reaction of PASP with Na_2S was greatly increased in the presence of H_2O_2, although H_2O_2 alone cannot react with PASP. Molecular-orbital calculations show that PASP exists at three level transitions and is expected to be used as electron acceptors in polymer solar cells.

ASSOCIATED CONTENT

Supporting Information

Detailed procedure for purification of PASP. Figures S1 and S2 give the IR and ^1H NMR spectra. Figure S3 shows the plots of A^{0-0}, A^{0-1}, and A^{0-0}/A^{0-1} versus concentration of PASP. Figure S4 shows CV curves of PASP in aqueous solution at different scan rates. Figure S5 shows absorption spectra changes of PASP and Na_2S at different time in aqueous solution after vigorous shaking. Figure S6 shows absorption spectra changes of PASP in the presence of Na_2S and H_2O_2 aqueous solution at different time. Figure S7 shows EPR spectrum of monoanion radical $PASP^{-\bullet}$ in Na_2S aqueous solution in the presence of H_2O_2. Figure S8 is the first three excitations of the neutral PASP in gaseous phase. Table S1 and S2 give the calculated orbits' energies of PASP. This material is available free of charge via the Internet at http://pubs.acs.org/.

AUTHOR INFORMATION

Corresponding Author

*E-mail: xff@shu.edu.cn (F.X.); shourongzhu@shu.edu.cn (S.Z.). Fax: +86-21-66134594.

Notes

The authors declare no competing financial interest.

ACKNOWLEDGMENTS

REFERENCES

(1) Kohl, C.; Weil, T.; Qu, J.; Muellen, K. Chem.—Eur. J. 2004, 10, 5297−5310.

(2) Schmidt, C. D.; Böttcher, C.; Hirsch, A. Eur. J. Org. Chem. 2009, 2009, 5337−5349.

(3) Langhals, H. Helv. Chim. Acta 2005, 88, 1309−1343.

(4) Li, L.; Guan, M.; Cao, G.; Li, Y.; Zeng, Y. Appl. Phys. A: Mater. Sci. Process 2010, 99, 251−254.

(5) Ren, H.; Li, J.; Wang, R.; Zhang, T.; Gao, Z.; Liu, D. Polymer 2011, 52, 3639−3646.

(6) Barra, M.; Di Girolamo, F. V.; Chiarella, F.; Salluzzo, M.; Chen, Z.; Facchetti, A.; Anderson, L.; Cassinese, A. J. Phys. Chem. C 2010, 114, 20387−20393.

(7) Bonavolontà, C.; Albonetti, C.; Barra, M.; Valentino, M. J. Appl. Phys. 2011, 110, 093716.

(8) Feng, X.; An, Y.; Yao, Z.; Li, C.; Shi, G. ACS Appl. Mater. Interfaces 2012, 4, 614−618.

(9) Hu, Y.; Wang, K.; Zhang, Q.; Li, F.; Wu, T.; Niu, L. Biomaterials 2012, 33, 1097−1106.

(10) Huang, L.; Tam-Chang, S. -W. Chem.Commun. 2011, 47, 2291−2293.

(11) Hiromitsu, I.; Murakami, Y.; Ito, T. Synth. Met. 2003, 137, 1385−1386.

(12) Lane, P. A.; Rostalski, J.; Giebeler, C.; Martin, S. J.; Bradley, D. D. C.; Meissner, D. Sol. Energy Mater. Sol. Cells 2000, 63, 3−13.

(13) Hüttner, S.; Sommer, M.; Thelakkat, M. Appl. Phys. Lett. 2008, 92, 093302.

(14) Ambrosek, D.; Marciniak, H.; Lochbrunner, S.; Tatchen, J.; Li, X. Q.; Würthner, F.; Kühn, O. Phys. Chem. Chem. Phys. 2011, 13, 17649−17657.

(15) Bahng, H. W.; Yoon, M. C.; Lee, J. E.; Murase, Y.; Yoneda, T.; Shinokubo, H.; Osuka, A.; Kim, D. J. Phys. Chem. B 2012, 116, 1244−1255.

(16) Flamigni, L.; Zanelli, A.; Langhals, H.; Böck, B. J. Phys. Chem. A 2012, 116, 1503−1509.

(17) Georgiev, N. I.; Sakr, A. R.; Bojinov, V. B. Dyes Pigm. 2011, 91, 332−339.

(18) Gunderson, V. L.; Krieg, E.; Vagnini, M. T.; Iron, M. A.; Rybtchinski, B.; Wasielewski, M. R. J. Phys. Chem. B 2011, 115, 7533−7540.

(19) Manning, S. J.; Bogen, W.; Kelly, L. A. J. Org. Chem. 2011, 76, 6007−6013.

(20) Ramanan, C.; Smeigh, A. L.; Anthony, J. E.; Marks, T. J.; Wasielewski, M. R. J. Am. Chem. Soc. 2012, 134, 386−397.

(21) Suzuki, S.; Kozaki, M.; Nozaki, K.; Okada, K. J. Photochem. Photobiol., C 2011, 12, 269−292.

(22) Wu, W.; Guo, H.; Wu, W.; Ji, S.; Zhao, J. J. Org. Chem. 2011, 76, 7056−7064.

(23) Zhao, Y.; Sun, J.; Shi, Z.; Pan, C.; Xu, M. Luminescence 2011, 26, 214−217.

(24) Zhu, L.; Jiao, C.; Xia, D.; Wu, J. Tetrahedron Lett. 2011, 52, 6411−6414.

(25) Yukruk, F.; Lale Dogan, A.; Canpinar, H.; Guc, D.; Akkaya, E. U. Org. Lett. 2005, 7, 2885−2887.

(26) Würthner, F. Chem. Commun. 2004, 1564−1579.

(27) Xu, Y.; Leng, S.; Xue, C.; Sun, R.; Pan, J.; Ford, J.; Jin, S. Angew. Chem, Int. Ed. 2007, 46, 3896−3899.

(28) Yamamoto, M.; Wang, S.; Jiang, Z.; Ramirez, R. Patent WO2010/099214 A1, 2010.

(29) Gao, B.; Li, H.; Liu, H.; Zhang, L.; Bai, Q.; Ba, X. Chem.Commun. 2011, 47, 3894−3896.

(30) Gao, B.; Xia, D.; Zhang, L.; Bai, Q.; Bai, L.; Yang, T.; Ba, X. J. Mater. Chem. 2011, 21, 15975−15980.

(31) Cakır, D.; Gülseren, O.; Mete, E.; Ellialtıroglu, S. J. Phys. Chem. C 2011, 115, 9220−9226.

(32) Mete, E.; Uner, D.; Cakmak, M.; Gulseren, O.; Ellialtŏlu, S. J. Phys. Chem. C 2007, 111, 7539−7547.

(33) Ozcan, O.; Yukruk, F.; Akkaya, E. U.; Uner, D. Top. Catal. 2007, 44, 523−528.

(34) Tuntiwechapikul, W.; Taka, T.; Béthencourt, M.; Makonkawkeyoon, L.; Randall Lee, T. Med. Chem. Lett. 2006, 16, 4120−4126.

(35) Sun, Y.; Li, Z.; Wang, Z. J. Mater. Chem. 2012, 22, 4312−4318.

(36) Tauber, M. J.; Kelley, R. F.; Giaimo, J. M.; Rybtchinski, B.; Wasielewski, M. R. J. Am. Chem. Soc. 2006, 128, 1782−1783.

(37) Marcon, R. O.; Brochsztain, S. J. Phys. Chem. A 2009, 113, 1747−1752.

(38) Che, Y.; Datar, A.; Yang, X.; Naddo, T.; Zhao, J.; Zang, L. J. Am. Chem. Soc. 2007, 129, 6354−6355.

(39) Marcon, R. O.; Brochsztain, S. Langmuir 2007, 23, 11972−11976.

(40) Marcon, R. O.; dos Santos, J. G.; Figueiredo, K. M.; Brochsztain, S. Langmuir 2006, 22, 1680−1687.

(41) Frisch, M. J.; Trucks, G. W.; Schlegel, H. B.; Scuseria, G. E.; Robb, M. A.; Cheeseman, J. R.; Montgomery, J. A., Jr.; Vreven, T.; Kudin, K. N.; Burant, J. C.; Millam, J. M.; Iyengar, S. S.; Tomasi, J.; Barone, V.; Mennucci, B.; Cossi, M.; Scalmani, G.; Rega, N.; Petersson, G. A.; Nakatsuji, H.; Hada, M.; Ehara, M.; Toyota, K.; Fukuda, R.; Hasegawa, J.; Ishida, M.; Nakajima, T.; Honda, Y.; Kitao, O.; Nakai, H.; Klene, M.; Li, X.; Knox, J. E.; Hratchian, H. P.; Cross, J.

3406

dx.doi.org/10.1021/am4004446 | ACS Appl. Mater. Interfaces 2013, 5, 3401−3407

B.; Bakken, V.; Adamo, C.; Jaramillo, J.; Gomperts, R.; Stratmann, R. E.; Yazyev, O.; Austin, A. J.; Cammi, R.; Pomelli, C.; Ochterski, J. W.; Ayala, P. Y.; Morokuma, K.; Voth, G. A.; Salvador, P.; Dannenberg, J. J.; Zakrzewski, V. G.; Dapprich, S.; Daniels, A. D.; Strain, M. C.; Farkas, O.; Malick, D. K.; Rabuck, A. D.; Raghavachari, K.; Foresman, J. B.; Ortiz, J. V.; Cui, Q.; Baboul, A. G.; Clifford, S.; Cioslowski, J.; Stefanov, B. B.; Liu, G.; Liashenko, A.; Piskorz, P.; Komaromi, I.; Martin, R. L.; Fox, D. J.; Keith, T.; Al-Laham, M. A.; Peng, C. Y.; Nanayakkara, A.; Challacombe, M.; Gill, P. M. W.; Johnson, B.; Chen, W.; Wong, M. W.; Gonzalez, C.; Pople, J. A. *Gaussian 03*, Revision C.2; Gaussian, Inc.: Wallingford, CT, 2003.

(42) Bauernschmitt, R.; Ahlrichs, R. *Chem. Phys. Lett.* **1996**, *256*, 454−464.

(43) Li, A. D. Q.; Wang, W.; Wang, L. Q. *Chem.—Eur. J.* **2003**, *9*, 4594−4601.

(44) Backes, C.; Schmidt, C. D.; Rosenlehner, K.; Hauke, F.; Coleman, J. N.; Hirsch, A. *Adv. Mater.* **2010**, *22*, 788−802.

(45) Ma, Y.; Wu, J.; Chang, N.; Sun, S. *Huaxue Chuanganqi* **2010**, *30*, 65−68.

(46) Shoukry, A. A. *J. Solution Chem.* **2011**, *40*, 1796−1818.

(47) Chen, J.; Shi, M. M.; Hu, X. L.; Wang, M.; Chen, H. Z. *Polymer* **2010**, *51*, 2897−2902.

(48) Schmidt, R.; Ling, M. M.; Oh, J. H.; Winkler, M.; Könemann, M.; Bao, Z.; Würthner, F. *Adv. Mater.* **2007**, *19*, 3692−3695.

(49) Calzado, E. M.; Villalvilla, J. M.; Boj, P. G.; Quintana, J. A.; Gómez, R.; Segura, J. L.; Díaz-García, M. A. *J. Phys. Chem. C* **2007**, *111*, 13595−13605.

(50) Bullock, J. E.; Vagnini, M. T.; Ramanan, C.; Co, D. T.; Wilson, T. M.; Dicke, J. W.; Marks, T. J.; Wasielewski, M. R. *J. Phys. Chem. B* **2010**, *114*, 1794−1802.

(51) Lee, S. K.; Zu, Y.; Herrmann, A.; Geerts, Y.; Müllen, K.; Bard, A. J. *J. Am. Chem. Soc.* **1999**, *121*, 3513−3520.

(52) Gosztola, D.; Niemczyk, M. P.; Svec, W. *J. Phys. Chem. A* **2000**, *104*, 6545−6551.

(53) Ford, W. E.; Hiratsuka, H.; Kamat, P. V. *J. Phys. Chem.* **1989**, *93*, 6692−6696.

(54) Penneau, J. F.; Stallman, B. J.; Kasai, P. H.; Miller, L. L. *Chem. Mater.* **1991**, *3*, 791−796.

(55) Miller, L. L.; Mann, K. R. *Acc. Chem. Res.* **1996**, *29*, 417−423.

(56) Slater, B. J.; Davies, E. S.; Argent, S. P.; Nowell, H.; Lewis, W.; Blake, A. J.; Champness, N. R. *Chem.—Eur. J.* **2011**, *17*, 14746−14751.

(57) Goretzki, G.; Davies, E. S.; Argent, S. P.; Alsindi, W. Z.; Blake, A. J.; Warren, J. E.; McMaster, J.; Champness, N. R. *J. Org. Chem.* **2008**, *73*, 8808−8814.

(58) Chamberlain, T. W.; Davies, E. S.; Khlobystov, A. N.; Champness, N. R. *Chem.—Eur. J.* **2011**, *17*, 3759−3767.

(59) Perrin, L.; Hudhomme, P. *Eur. J. Org. Chem.* **2011**, *2011*, 5427−5440.